Biophysical and Biogeochemical Responses to Climate Change Depend on Dispersal and Migration

PAUL A. T. HIGGINS AND JOHN HARTE

Different species, populations, and individuals disperse and migrate at different rates. The rate of movement that occurs in response to changes in climate, whether fast or slow, will shape the distribution of natural ecosystems in the decades to come. Moreover, land-use patterns associated with urban, suburban, rural, and agricultural development will complicate ecosystem adaptation to climate change by hindering migration. Here we examine how vegetation's capacity to disperse and migrate may affect the biophysical and biogeochemical characteristics of the land surface under anthropogenic climate change. We demonstrate that the effectiveness of plant migration strongly influences carbon storage, evapotranspiration, and the absorption of solar radiation by the land surface. As a result, plant migration affects the magnitude, and in some cases the sign, of feedbacks from the land surface to the climate system. We conclude that future climate projections depend on much better understanding of and accounting for dispersal and migration.

Keywords: vegetation–climate feedback, global change, carbon storage, evapotranspiration, surface radiation

Biological systems have responded to 20th-century changes in climate with range shifts and alterations in the timing of key life events, such as flowering, bud burst, and seasonal migration patterns (Parmesan and Yohe 2003, Root et al. 2003). The climate changes expected over the next 100 years exceed those of the past century (IPCC 2001) and are likely to lead to additional range shifts as the narrow climate characteristics required by many individuals, populations, and species move throughout the world. How successfully biological systems shift their ranges will depend on the rate and magnitude of climate changes to come and on the rate at which species are able to migrate in response to those climate changes.

Fossil pollen data from the early Holocene have been widely interpreted to demonstrate that long-lived plant species migrated extremely quickly in response to postglacial warming: up to 100 to 1000 meters (m) per year (10 to 100 kilometers per century) for tree species (Higgins and Richardson 1999, Tinner and Lotter 2001). Pollen analysis cannot accurately map present-day tree ranges, however, in part because the approach used to analyze pollen does not account for extensive areas where species exist at low densities (McLachlan and Clark 2004). Furthermore, lodgepole pine is still expanding northward, which demonstrates that the species is not yet in equilibrium with climate after a minimum of 300 to 400 years (Johnstone and Chapin 2003). Such findings suggest that the estimates of rapid migration in the past may be overly optimistic.

Similarly, results from diffusion models lead to somewhat ambiguous conclusions about migration rates. Recent advances in model development, such as the inclusion of the potential for occasional long-distance dispersal, help explain how migration rates could be fast (Clark 1998). On the other hand, the inclusion of potentially realistic model assumptions, such as discrete individuals and stochasticity, leads to spread rates that appear to be much slower (Clark et al. 2003). These contradictory interpretations suggest that scientists really do not yet know how rapidly vegetation can migrate in response to changes in climate.

Furthermore, the large and rapid climate changes expected over the next century, even under moderate greenhouse gas (GHG) emissions scenarios (IPCC 2001), would require much faster rates of species migration than those optimistically supposed for postglacial warming (Solomon and Kirilenko 1997, Malcolm et al. 2002). Yet migration rates

Paul A. T. Higgins (e-mail: phiggins@nature.berkeley.edu), formerly a visiting research fellow at the University of California, Berkeley, is now an AMS/UCAR (American Meteorological Society/University Corporation for Atmospheric Research) Congressional Science Fellow. John Harte (e-mail: jharte@berkeley.edu) is a professor at the University of California, Berkeley, CA 94720.

(and our ability to predict migration patterns) are inherently uncertain even for undisturbed conditions (Clark et al. 2003). Land-use patterns associated with urban, suburban, rural, and agricultural development very likely further complicate ecosystem adaptation to climate change by hindering migration.

The ability of biological systems to migrate and disperse in response to climate change will also depend on the magnitude and rate at which climate changes occur over the next century and beyond. Larger changes in climate imply the need for species to migrate longer distances. A broad range of GHG emissions scenarios are now considered possible for the next century (Nakicenovic et al. 2000), leading to a range in expected globally averaged temperature increases of 1.4 degrees Celsius (°C) to 5.8°C by the year 2100 (IPCC 2001). At the low end of the range of projected GHG emissions, such as the B1 scenario (see *www.grida.no/climate/ipcc_tar/wg1/008.htm*), atmospheric carbon dioxide (CO_2) would increase to roughly 550 parts per million (ppm) by 2100, relative to roughly 280 ppm under preindustrial conditions (IPCC 2001). The increase in radiative forcing associated with GHG concentrations under the B1 scenario (see *www.ipcc.ch/pub/taroldest/wg3/015.htm*) is roughly 4.2 watts (W) per m^2, which leads to predicted increases in globally averaged annual temperature toward the lower end of the expected range. At the high end of the GHG emissions scenarios, the A1FI scenario (*www.ipcc.ch/pub/taroldest/wg3/015.htm*) would lead to CO_2 concentrations of roughly 1000 ppm by 2100. This translates into an increase of roughly 9.1 W per m^2 in globally averaged radiative forcing, and predicted temperature increases at the high end of the expected range.

Under the A1FI emissions scenario, the HadCM3 climate model projects large increases in annually averaged temperature throughout the world (1°C to 11°C) and some substantial regional shifts in precipitation relative to a control simulation using preindustrial GHG concentrations (Johns et al. 2003). Changes in annually averaged temperature are largest in the high latitudes and in parts of northern South America (6°C to 11°C). Large changes in precipitation also occur, with increases primarily in the high latitudes and both gains and losses occurring in the tropics. The Amazon region of South America, in particular, gets much drier under the A1FI scenario, while precipitation increases in parts of Southeast Asia.

Even for the lower emissions scenarios, the resulting climate changes may occur more rapidly than those witnessed over the last several decades, suggesting that some tree species will be unable to fully occupy their future ranges for years to come. The changes predicted under the higher emissions scenarios, such as A1FI, would be likely to trigger a massive shift in the distribution of vegetation.

The biological responses to these climate changes, in turn, will contribute important feedbacks to the climate system by altering biophysical and biogeochemical characteristics of the land surface. For example, changes in the distribution of vegetation can alter carbon storage, land-surface albedo, surface roughness, and evapotranspiration (Betts et al. 1997, Lashof et al. 1997, Sellers et al. 1997, Field and Avissar 1998, Pielke et al. 1998, Saleska et al. 2002, Feddema et al. 2005). The effectiveness of plant migration has been shown to influence terrestrial carbon storage (van Minnen et al. 2000) and could influence these important climate feedbacks at local, regional, or global scales (Chapin et al. 2005).

Furthermore, the assumption that all individuals of a species share the same climate requirements, rather than occupy distinct population-level climate envelopes, may underestimate the number of individuals within a species that need to migrate under climate change. The reason is that local adaptations may lead to more narrow climate requirements for populations than would be implied by the full species range (Harte et al. 2004). Individuals and populations currently residing at the northern boundary of a species range may be ill suited to the climate characteristics that other individuals and populations of the same species thrive in at the southern boundary. If so, species ranges are more constrained than has been widely recognized, as migration needs will be specific to the smaller spatial distributions of individuals and populations rather than to ranges of whole species.

Therefore, impact assessment and prediction of future climate conditions depend on understanding how effectively biological systems will migrate in response to changes in climate. Here we examine how migration may affect biological responses to climate change using the Integrated Biosphere Simulator (IBIS; Foley et al. 1996, Kucharik et al. 2000). We test a range of plausible migration assumptions for vegetation to determine biophysical and biogeochemical responses of the land surface to the A1FI climate scenario, as modeled by HadCM3 (Johns et al. 2003).

Ecosystem model and climate input

We developed two climate scenarios to test the importance of plant migration in determining broadscale structural and functional ecosystem responses to climate change. The two climate scenarios are based on HadCM3-derived monthly climate averages for temperature, precipitation, relative humidity, and wind speed over a 20-year period corresponding to 2081–2100 under (a) control, or preindustrial, GHG concentrations (Johns et al. 2003) and (b) the A1FI emissions scenario (described above). The study of ecosystem responses, described below, also requires climate scenarios to include the monthly average temperature range, cloudiness, and number of rainy days, which are not available to us from the HadCM3. Therefore, we combined the model data for each scenario with monthly average temperature range, cloudiness, and number of rainy days from historical climatology between 1961 and 1990 (New et al. 1999).

To test ecosystem structure and function under each climate scenario, we used IBIS 2.6, a process-based, dynamic global ecosystem model (Foley et al. 1996, Kucharik et al. 2000). IBIS is designed to run alone (i.e., using fixed external climate conditions as input) or coupled to a general circulation model to allow feedbacks from the land surface to alter the physics

of the atmosphere. We used uncoupled simulations to reduce technical and computational demands and because validation studies are more extensive for uncoupled simulations. Using uncoupled simulations allowed us to determine the land-surface responses to the climate change scenario but did not allow the closing of the feedback loops between the land surface and the atmosphere. Including these feedbacks would alter climate and therefore further alter the land-surface response. Thus, our results should be viewed not as predictive but as a first step to determining and quantifying the importance of migration to biophysical and biogeochemical responses of the land surface.

The IBIS simulations described below use a spatial resolution of 2.5° latitude by 3.75° longitude, which matches the spatial resolution of HadCM3. IBIS also requires daily and hourly climate conditions, which are produced by an internal weather generator that converts the monthly climate input. In addition to the monthly climate data described above, IBIS requires input data for topography and soil texture (GSDTG 2000).

IBIS represents vegetation in broad categories or plant functional types (PFTs) that differ in basic form (trees, shrubs, or grasses), leaf type (broadleaf or needleleaf), patterns of leaf display (evergreen or deciduous), and photosynthetic pathway (C_3 or C_4). IBIS uses leaf-level calculations for photosynthesis (Farquhar et al. 1980, Collatz et al. 1991, 1992), respiration, and stomatal conductance (Foley et al. 1996, Kucharik et al. 2000) to determine instantaneous carbon and water balances at an hourly time step. Seasonal changes in climate, light availability, and patterns of leaf display alter rates of photosynthesis, respiration, and stomatal conductance throughout the year. Annual carbon balance for each PFT is determined by integrating these hourly measurements over the entire year, and used to measure net primary productivity (NPP), the relative success of different PFTs, and the availability of carbon for each PFT to allocate to the growth of additional root, stem, and leaf material.

Under different climate conditions, the characteristics of each PFT can be more or less favorable for photosynthesis and respiration. In general, trees, shrubs, and grasses compete for light and water, with trees better able to capture light first and shrubs and grasses better able to access water in the upper soil layers, but PFTs also differ in their ability to take up and respire carbon (as a function of leaf form, seasonal patterns of leaf display, and photosynthetic pathway).

Climate characteristics also influence soil carbon, which depends on inputs from litter fall and root turnover and on transformations between four soil carbon pools. The four carbon pools include (1) an active pool that has residence times in the range of hours to months (i.e., microbial biomass), (2 and 3) slow pools with residence times of 10 to 30 years (i.e., protected and unprotected organic matter), and (4) a recalcitrant pool with residence times of more than 1000 years (i.e., stabilized organic matter). Increases in soil temperature or moisture generally increase rates of organic matter decomposition and increase transformations between soil carbon pools. Climate changes can also influence the amount of carbon entering the soil as litter and root turnover by altering plant community composition and NPP.

Migration scenarios

In the canonical or standard form of IBIS (Foley et al. 1996, Kucharik et al. 2000), all PFTs are free to occur in and expand to any location, as long as climate conditions are favorable for them there. We altered this characteristic of the model to develop five plausible migration assumptions for vegetation and conduct a sensitivity study of biophysical and biogeochemical responses to these assumptions. The migration assumptions include (a) MAX, in which all PFTs can move freely to any location where climate becomes favorable (the canonical form of IBIS); (b) MIN, in which established vegetation dies when climate becomes unfavorable for it, but no PFT can expand in locations that become more favorable under climate change; (c) LOCAL, in which vegetation types can expand within any grid cell in which they were previously established, but no PFT can move to new locations; (d) G&S FREELY, in which grasses and shrubs can migrate to any grid cell in the world, but tree PFTs cannot move anywhere they were not previously established; and (e) NEIGHBORS, in which trees can move from any cell where they were previously established to any neighboring cell, while grasses and shrubs are free to migrate anywhere.

Each of the constrained migration assumptions is generated through imposed limits on PFT movement between model grid cells. The model grid cell boundaries we used to impose migration limits have nothing to do with actual migration patterns, routes, or barriers that organisms face. Instead, migration distances were constrained nonmechanistically to the size of our grid cells (2.5° latitude by 3.75° longitude), a simple and intuitive way to describe limited migration distances. We also included a single simulation using the canonical version of IBIS (i.e., with unconstrained PFT distributions) under the control climate scenario. This provided the original distribution of vegetation and allowed us to distinguish and compare ecosystem responses due to the climate change from those due to the different migration assumptions. We then quantified the biophysical and biogeochemical responses under each assumption.

Except for the MIN assumption, each IBIS simulation begins from a cold start (i.e., without previously established vegetation patterns) but with the restrictions limiting where PFTs can occur in each of the constrained migration simulations described above. The MIN simulation was created by taking the smaller of the two biomass values from the control or MAX simulation for each PFT. We then held that biomass constant throughout the simulation. We ran the control and five A1FI simulations for 200 years by repeating the annual climate patterns for each scenario. This revealed near-equilibrium ecosystem structure and function for each migration assumption but provided no insights into transient responses. In order to isolate ecosystem responses to climate change from physiological responses to CO_2 enrichment, we

held atmospheric CO_2 concentrations at 350 ppm for all IBIS simulations.

Comparative analysis

We compared annual NPP, carbon storage in biomass and soil, absorbed solar radiation, and changes in latent heat flux among the different migration assumptions by averaging over the final decade of each IBIS simulation. We also determined the potential biome distribution under the control and MAX simulations by averaging leaf area index (LAI) for each PFT over the final decade and then applying the IBIS annual biome classification scheme. The classification scheme distinguishes among biomes on the basis of a grid cell's total LAI, its dominant PFT (i.e., the one with the largest contribution to LAI), and the combination of other PFTs that occur in the grid cell (Foley et al. 1996, Kucharik et al. 2000). Averaging over the last decade reduces the potential for interannual variability caused by the weather generator.

We compared changes in mean annual latent heat flux throughout the world for the constrained migration simulations, with differences determined by *t* test. The *t* test is appropriate if we assume that vegetation responses are not influenced by longer-term memory of the interannual variability introduced by the weather generator.

Our estimates for absorbed solar radiation at the land surface (R) are based on midday direct-beam land-surface albedo (data not shown) and calculated as follows:

$$R = S_{grnd} \times (1 - \alpha_T), \quad (1)$$

where S_{grnd} is the amount of solar radiation reaching the land surface and α_T is the land-surface albedo. IBIS calculates land-surface albedo using a two-stream approximation for visible and near-infrared wave bands (Foley et al. 1996, Kucharik et al. 2000). Snow characteristics (depth, temperature, age, and whether on the ground or in the canopy), soil moisture, LAI, and canopy height determine land-surface albedo. We determine total direct beam land-surface albedo by summing the visible and infrared fractions, as previously described (Higgins 2004). S_{grnd} varies by latitude and season and is calculated locally as

$$S_{grnd} = S_0 \times \cos Z \times (1 - \alpha_{atm} - ß_{atm}), \quad (2)$$

where S_0 is the solar constant (1366 W per m^2); cos Z is the cosine of the zenith angle, calculated as described by Washington and Parkinson (1986); α_{atm} is the atmospheric albedo; and $ß_{atm}$ is the fraction of direct-beam solar radiation absorbed by the atmosphere. Although α_{atm} and $ß_{atm}$ vary because of an uneven distribution of clouds (Kiehl and Trenberth 1997), this calculation holds them constant at their estimated global averages (0.23 and 0.20, respectively), since model data on cloud distributions are not available. As a result, our approach overestimates the solar radiation absorbed by the surface in areas with heavy cloud cover and underestimates surface radiation in areas with light cloud cover. Furthermore, this approach ignores potential changes in cloud cover that could alter the amount of solar radiation that reaches Earth's surface and thereby amplify or dampen changes. Nevertheless, this rough estimate of the change in absorbed radiation at the land surface provides a useful approximation of the importance of the vegetation's responses.

Biophysical and biogeochemical responses

Under the control climate scenario, potential biome distributions (figure 1a) agree broadly with reported potential biome distributions under historical climate patterns (Ramankutty and Foley 1999). Without migratory constraints, vegetation distributions shift throughout the world in response to the climate changes associated with the A1FI emissions scenario (figure 1b). Most notably, large losses of forest occur in the Amazonian region of South America, where precipitation decreases in HadCM3 under the A1FI emissions scenario. In the high northern latitudes, boreal forest expands into regions previously occupied by tundra vegetation under the control climate scenario.

Barriers to migration alter potential biome distributions throughout the world relative to the distributions that occur under the MAX migration assumption (figure 2). Relative to unconstrained migration (MAX), vegetation under the MIN assumption is characterized by much greater areas of desert, where vegetation is largely absent (figure 2a). In the MIN simulation there is also a large loss of forest in northern Asia. If vegetation can expand locally (LOCAL assumption), the area of additional desert decreases, though not entirely (figure 2c). Large losses in forest area, particularly in the high latitudes, also occur under the LOCAL migration assumption, while a large area of forest in Asia shifts to being deciduous instead of the evergreen forest of the MAX migration assumption. Unconstrained grass and shrub migration (G&S FREELY; figure 2b), relative to the MAX assumption, has considerably less forested area in the high latitudes and in parts of South America, where tree PFTs were rare under the control climate. Allowing tree PFTs to migrate to any neighboring cell (NEIGHBORS) further reduces differences in biome distribution, with only those remote forested areas, primarily in the high latitudes, differing from those of the MAX migration assumption (figure 2d).

NPP under the control climate is roughly 65 petagrams (Pg) of carbon per year. This is within the range estimated under current conditions, but at the high end of the range (Cramer et al. 1999). NPP under all migration assumptions declines sharply under the A1FI climate scenario (figure 3), leading to a loss of nearly 15 Pg of carbon per year even with unconstrained migration (MAX). The ability of vegetation to migrate and disperse in response to the A1FI climate changes does strongly influence NPP, with the MIN migration assumption leading to an additional loss of 20 Pg of carbon per year relative to the MAX migration assumption. Allowing PFTs to respond within any cell where they are previously established (LOCAL) allows NPP to recover nearly half of the carbon lost in the MIN migration simulation. The G&S FREELY and NEIGHBORS assumptions lead to NPP levels nearly equal to those of the MAX migration simulation, suggesting that PFTs

can generally take advantage of available light and water even if they are not completely adapted for the local climate conditions in which they exist.

Modeled carbon storage in live biomass and in the soil (table 1) under the control climate falls within the range of existing estimates (Jobbagy and Jackson 2000, IPCC 2001), with roughly 715 and 1688 Pg of carbon stored in biomass and soil, respectively. Not surprisingly given the large changes in NPP, the change in climate associated with the A1FI climate scenario also leads to a large change in carbon storage. Indeed, with a minimum loss of more than 800 Pg of stored carbon, the magnitude of lost carbon storage exceeds the total current atmospheric carbon pool under all migration scenarios. Even larger losses in terrestrial carbon storage occur in the simulations with constrained migration. For example, lost carbon storage under the MIN assumption, relative to MAX, equals roughly 450 Pg, while the carbon lost under the LOCAL migration assumption equals roughly 309 Pg. Both exceed the total cumulative carbon emissions due to fossil fuel burning and cement production for the entire world since the start of the Industrial Revolution (Marland et al. 2003). In general, less constrained migration leads to more carbon storage. For example, the G&S FREELY simulation results in 142 Pg less carbon storage than the MAX simulation, whereas NEIGHBORS lacks only 67 Pg of stored carbon relative to MAX (which is still nearly 10% of the atmospheric carbon stock).

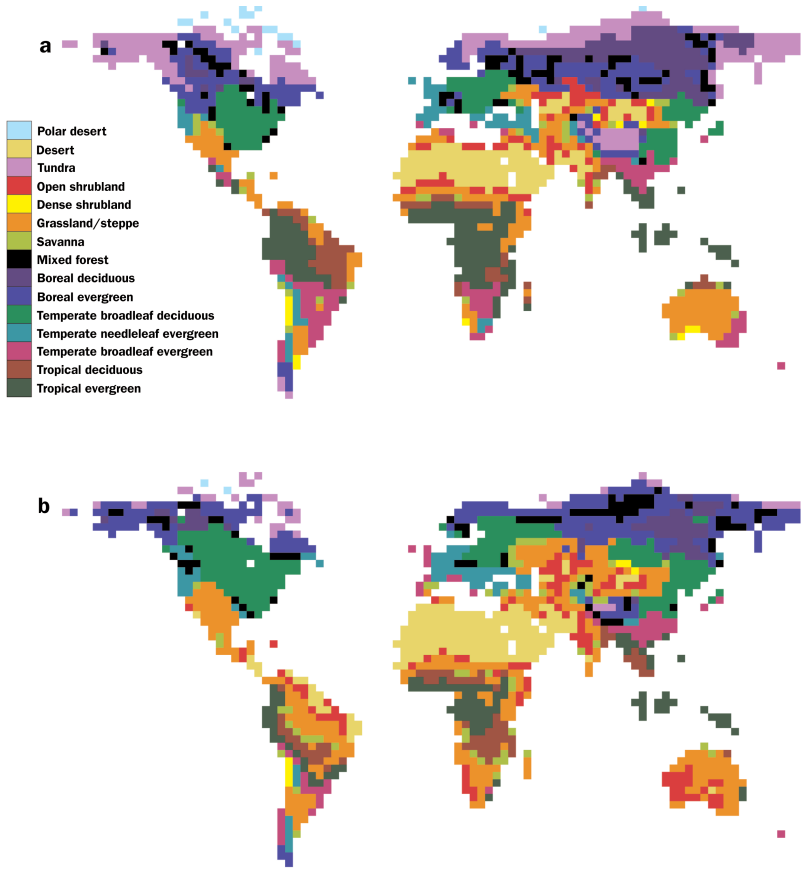

Figure 1. Simulated global biome distribution under (a) control and (b) A1FI climate scenarios. Biomes are determined using leaf area index for each plant functional type averaged over the final 10 years of the 200-year simulation. In each of these simulations, plant migration is unconstrained.

The amount of solar radiation absorbed by the land surface changes with the climate scenario and the migration assumption. Changes occur in latitude-specific ways, but with particularly strong changes occurring in high latitudes (figure 4). Between 44° north (N) and 61° N, absorbed solar radiation increases or decreases relative to that of the control simulation, depending on how vegetation migrates in response to the A1FI climate change scenario. Under the MAX migration assumption, absorbed solar radiation increases slightly throughout the latitude band, with larger increases at higher latitudes (up to 9.6 W per m^2). In contrast, absorbed solar radiation in the G&S FREELY and NEIGHBORS simulations decreases relative to that of the control throughout this latitude range (up to –8.6 W per m^2 and –5.9 W per m^2, respectively), which is consistent with reductions in tree LAI that occur in these simulations (data not shown). As a result, the sign of the vegetation–albedo feedback switches between positive and negative, depending on how effectively vegetation can migrate in response to the climate change.

At latitudes higher than 61° N, absorbed solar radiation increases for all migration assumptions relative to absorbed solar radiation under the control climate. Intuitively, this makes sense, since increasing temperatures at high latitudes lead to a decrease in snow and ice cover, which is a positive feedback to warming. The magnitude of this feedback depends heavily on the migration assumption, however, demonstrating that much of the increase in absorbed solar radiation is determined by vegetation responses and is not simply due to the ice–albedo feedback. For example, unconstrained tree migration (MAX) leads to

Table 1. Mean total global carbon storage in tissue and soil with standard deviations over the final 10 years of each IBIS simulation.

Assumption	Biomass carbon (petagrams)	Standard deviation	Soil carbon (petagrams)	Standard deviation
Control climate	715	0.19	1688	0.37
MAX	561	0.30	972	0.25
MIN[a]	274	0	810	1.79
LOCAL	405	0.09	819	0.23
G&S FREELY	390	0.15	1001	0.28
NEIGHBORS	485	0.17	980	0.26

a. Biomass carbon is fixed in the MIN simulation at the smaller of the two values from the control and MAX simulations for each plant functional type. As a result, the standard deviation = 0.

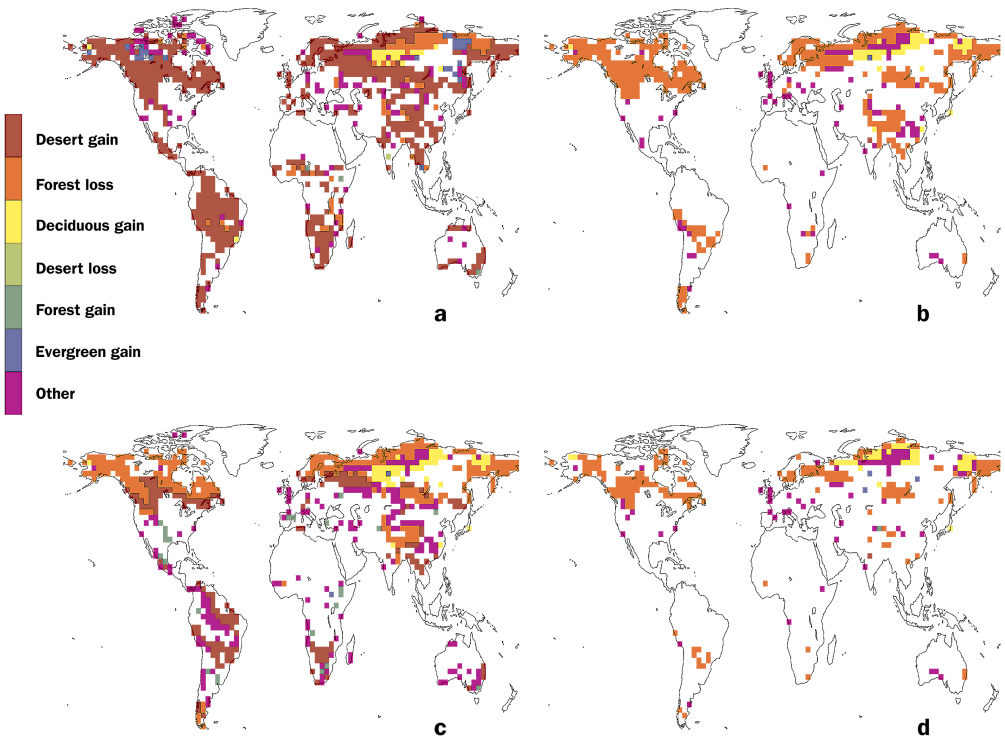

Figure 2. Global biome changes relative to the unconstrained migration simulation (MAX) for (a) MIN, (b) G&S FREELY, (c) LOCAL, and (d) NEIGHBORS migration assumptions. We aggregate the biome changes into seven broad categories: desert expansion, forest loss, conversion from evergreen to deciduous vegetation, desert loss, forest expansion, conversion from deciduous to evergreen vegetation, and all other changes.

a large increase in absorbed solar radiation above 63° N (from 7.6 to 25.2 W per m^2), whereas increases are considerably smaller for the G&S FREELY simulation, in which trees are unable to migrate to new locations (0.6 to 9.4 W per m^2), and the NEIGHBORS simulation, in which tree migration is limited to neighboring cells (4.5 to 15.4 W per m^2). Feedbacks of 15 to 25 W per m^2 are sufficiently large to cause substantially different climate and ecosystem combinations, such that accurate projection of future states requires fully coupled climate–ecosystem simulations. Nevertheless, it is clear that both the size and the sign of the vegetation–albedo feedback depend on the rates at which vegetation can migrate and disperse in response to climate change, but with responses that differ by latitude.

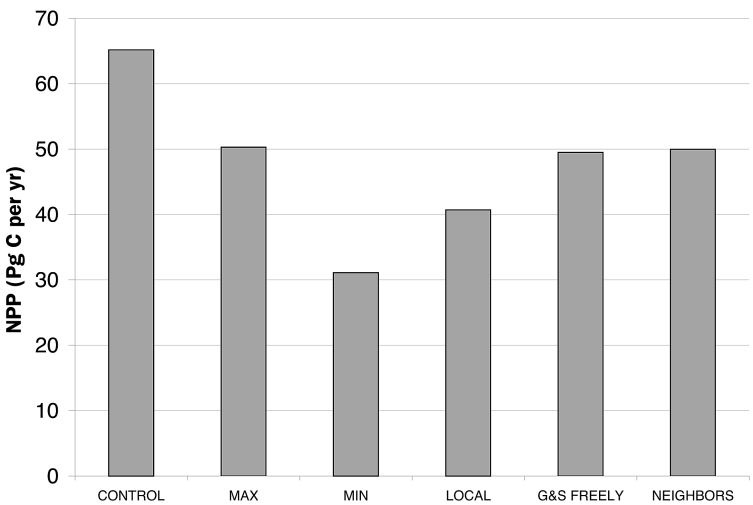

Figure 3. Globally aggregated net primary productivity (petagrams carbon per year) for each of the six IBIS scenarios.

Changes in the absorption of solar radiation also occur in South America (figure 5). Between 8.8° south (S) and 31° S, more heavily constrained migration leads to larger reductions in the absorption of solar radiation. For example, unconstrained tree migration (MAX) leads to changes in absorbed solar radiation from +0.4 to –6.1 W per m^2, whereas larger decreases occur for the G&S FREELY simulation, in which trees are unable to migrate to new locations (–3.9 to –9.2 W per m^2), and the NEIGHBORS simulation, in which tree migration is limited to neighboring cells (–2.1 to –6.2 W per m^2). Between 6° S and 11° N, absorbed solar radiation decreases from 2.7 to 7.8 W per m^2, relative to the control, for the migration assumptions, but with no differences

as a result of the migration assumption. This makes sense, since the loss of forest and soil drying that occurs in the region is identical under each of these migration assumptions. As with the higher latitude responses in the Northern Hemisphere described above, the size of the vegetation–albedo feedback (a negative feedback in South America) depends on the rates at which vegetation can migrate and disperse in response to climate change.

Dispersal and migration also influence the partitioning of net surface energy between sensible and latent heat fluxes. Under the MIN assumption, relative to MAX, large decreases in latent heat flux occur in the low and mid latitudes (figure 6a). This constitutes a large positive feedback to warming and drying, particularly within the tropics. For example, the warming and drying that occur in South America under the A1FI scenario lead to a reduction in latent heat flux. When vegetation is unable to migrate (MIN), additional losses of latent heat flux occur throughout the Amazon (up to 50 W per m^2 in some areas), a strong positive feedback to the initial warming and drying. In the LOCAL simulation, decreases in latent heat flux occur up to a similar magnitude but over a more limited area (figure 6c). This positive feedback decreases dramatically in the G&S FREELY simulation, however (down to less than 20 W per m^2 in all areas; figure 6b), and nearly disappears altogether under the NEIGHBORS assumption (figure 6d). Thus, migration can heavily influence the partitioning of energy between sensible and latent heat fluxes and the magnitude of this important climate feedback.

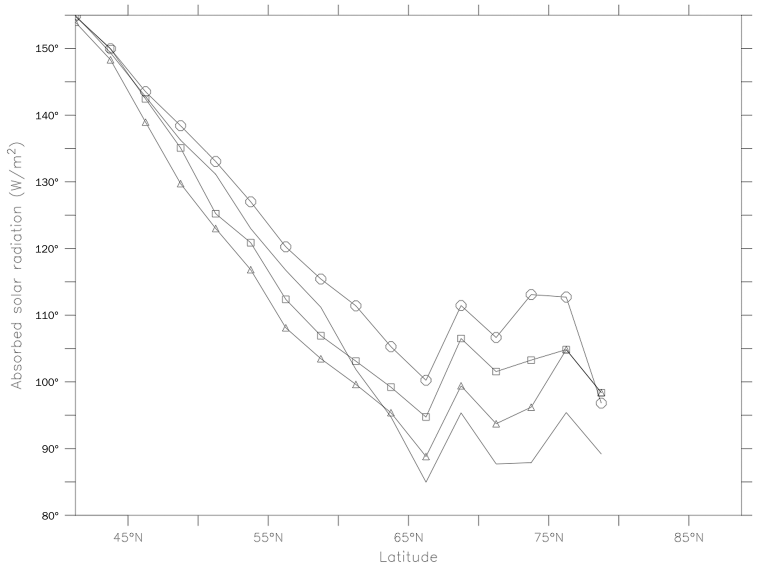

Figure 4. Zonal absorbed solar radiation north of 40° N for the control climate (line) and A1FI climate scenarios under the MAX (circles), G&S FREELY (triangles), and NEIGHBORS (squares) migration assumptions.

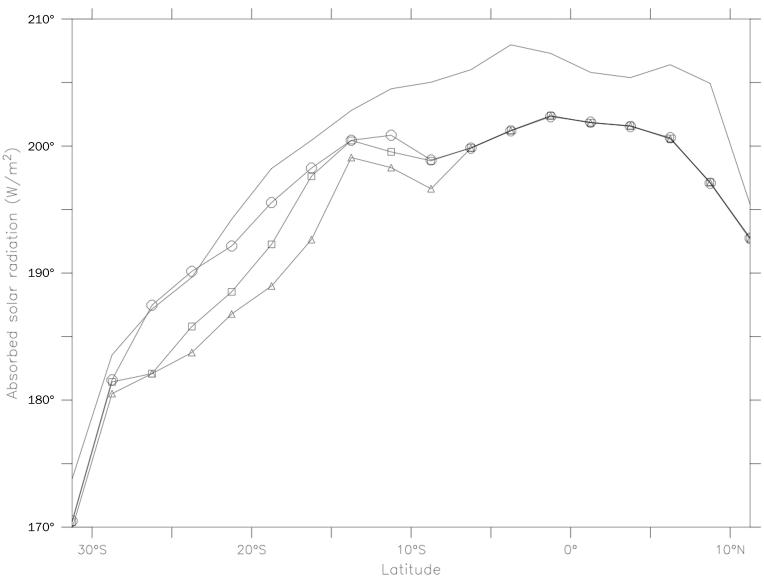

Figure 5. Absorbed solar radiation for South America between 8.8° S and 11° N for the control climate (line) and A1FI climate scenarios under the MAX (circles), G&S FREELY (triangles), and NEIGHBORS (squares) migration assumptions.

Implications and future needs

Biophysical and biogeochemical characteristics of the land surface affect climate by influencing carbon storage, land-surface albedo, and evapotranspiration (Betts et al. 1997, Lashof et al. 1997, Sellers et al. 1997, Field and Avissar 1998, Pielke et al. 1998, Saleska et al. 2002, Feddema et al. 2005). Results from our MAX migration simulation demonstrate that ecosystem responses to climate change can include important climate feedbacks even if plant migration is extremely fast.

For example, the difference in total stored carbon between the control and A1FI climate scenarios is more than 800 Pg, even if vegetation moves freely to wherever climate becomes most suitable. This carbon release from biomass and soil exceeds the current amount of carbon in the atmosphere and therefore constitutes a major positive feedback to climate warming. Indeed, if this amount of carbon were released from the land surface, the high CO_2 concentrations of the A1FI scenario would require much lower anthropogenic emissions than currently believed. This suggests that the potential for high GHG concentrations is also higher than widely recognized.

The large reduction in soil carbon evident under MAX migration most likely results from changes in both NPP and decomposition. The decreases in global NPP lead to smaller

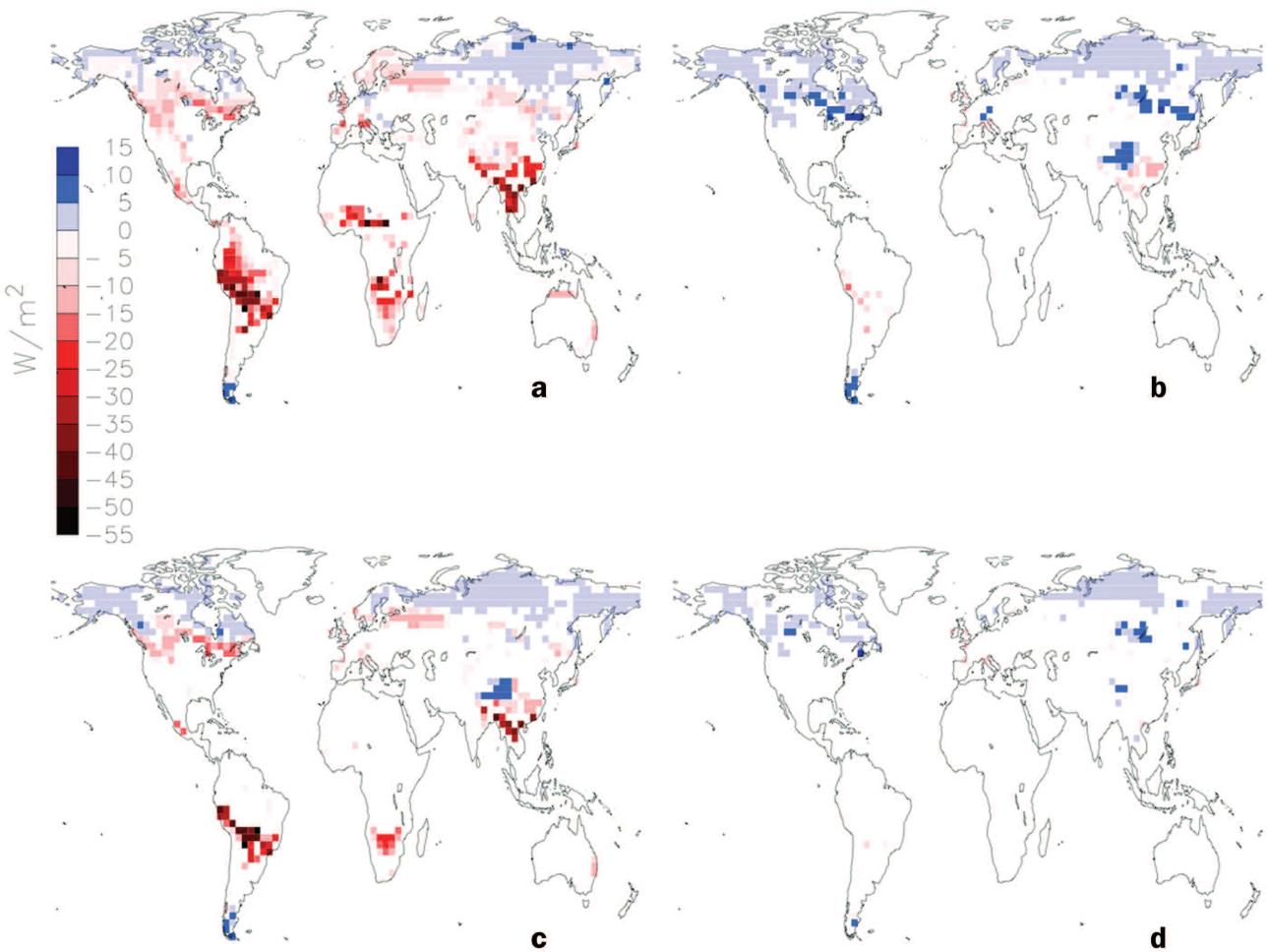

Figure 6. Change in latent heat flux, relative to unconstrained migration (MAX), for (a) MIN, (b) G&S FREELY, (c) LOCAL, and (d) NEIGHBORS migration assumptions. Only locations where significant changes occur are shown (P < 0.01 as measured by t test).

inputs of carbon from litter and root turnover. At the same time, higher temperatures in the A1FI scenario increase the speed of decomposition and reduce the residence time of carbon in soil and litter.

Important changes in land-surface albedo also occur under MAX migration, including a major positive feedback in the high northern latitudes and a moderate negative feedback in South America. The increase of 15 to 25 W per m^2 in absorbed solar radiation evident above 63° N is roughly double to triple the global mean radiative forcing due to A1FI emissions (approximately 9.1 W per m^2): a strong positive feedback to high-latitude warming.

Biological responses to climate change will also depend on how effectively species migrate to the locations where climate becomes most favorable to them. Even in the absence of land-use patterns, species-specific life history characteristics may slow or even preclude plant migration for at least some species or plant types. Land-use patterns associated with urban, suburban, rural, and agricultural development are likely to slow vegetation's ability to respond to climate change even further.

This examination of multiple plausible migration assumptions demonstrates that vegetation's capacity to disperse and migrate may lead to substantial additional feedbacks to the climate system. For example, under our more heavily constrained migration assumptions, terrestrial carbon losses can be as much as 1.4 to 1.5 times larger than the amount of carbon released if migration is unconstrained. As a result, carbon storage varies among the migration assumptions by more than the total historical emissions of carbon due to fossil fuel burning and cement production. Thus, heavily constrained migration leads to a strong additional positive feedback to warming through enhanced carbon release.

In some tropical areas, evapotranspiration also varies among the simulations, with increasingly strong positive feedbacks to warming and drying occurring as migration becomes more constrained. The decrease of 40 to 50 W per m^2 in latent heat flux that occurs under heavy migratory constraints is roughly 4 to 5 times the globally averaged

change in radiative forcing from A1FI emissions. Thus, the rate at which plants are able to migrate can lead to strong positive feedbacks at the local to regional scale by altering evapotranspiration. As with carbon storage, the strength of this positive feedback increases with more heavily constrained plant migration.

More heavily constrained migration can also weaken positive feedbacks or strengthen negative feedbacks, as illustrated by the changes in absorbed solar radiation. Above 61° N, the large increase in absorbed solar radiation shown in the MAX simulation decreases substantially: often by roughly 1/3 to 2/3 or more in the increasingly constrained G&S FREELY and NEIGHBORS simulations. At the same time, the negative feedback to warming evident in parts of South America increases with more heavily constrained migration. Interestingly, this feedback can be either positive or negative in the mid latitudes of the Northern Hemisphere, depending on how effectively vegetation is able to migrate. Thus, not only the magnitude but also the sign of feedbacks can, in some cases, depend on rates of migration and dispersal.

Together these responses illustrate that plant migration can have a powerful and complex impact on global and regional climate. Migratory constraints strengthen some feedbacks (e.g., carbon storage and latent heat fluxes) but weaken or even reverse others (e.g., absorbed solar radiation in the mid and high latitudes). Therefore, incorporating better understanding of migration into climate models will be necessary to project future climates accurately at global and regional scales.

It is important to recognize that this experiment is a sensitivity test rather than a mechanistic projection of future land-surface characteristics. A sensitivity test is a critical first step toward future projections because it demonstrates the importance of migration for biophysical and biogeochemical responses of the land surface. Future projections, however, will require a mechanistic treatment of migration and the inclusion of numerous factors that we ignore here. As has been previously noted, incorporating these advances into ecosystem models such as IBIS will be a difficult challenge (Neilson et al. 2005). Most notably, the use of model grid cell boundaries to impose migration limits is overly simplified, since grid cells have nothing to do with actual migration patterns, routes, or barriers that organisms face. Grid cells also have uniform climate conditions and therefore neglect the availability of microclimates that could act as refugia for PFTs and thereby decrease the distances that they must migrate. A further simplification is our use of a common migration assumption for PFTs, when actual species, populations, and individuals disperse and migrate at different rates. The failure of a species to migrate, for example, may allow the range expansion of competing species (Neilson et al. 2005). Nevertheless, basing migration assumptions on grid cell boundaries is a simple and intuitive way to describe limited migration distances and facilitates this sensitivity test of a range of plausible migration assumptions.

We note also that these results demonstrate only that migration is important in determining static biological responses to a single climate change scenario. We do not examine dynamic responses or interactions with other global changes, such as the direct effects of CO_2 enrichment, nitrogen deposition, land-use patterns, and exotic species invasions, all of which can alter biophysical and biogeochemical responses of the land surface.

In particular, physiological responses to elevated CO_2 concentrations are likely to affect ecosystem structure and function by altering rates of photosynthesis, respiration, and water-use efficiency (Mooney et al. 1999, Korner 2000). Incorporating the most widely demonstrated plot-level responses to CO_2 enrichment (Nowak et al. 2004, Norby et al. 2005) into model simulations would most likely lead to decreased plant water stress and increased NPP and carbon storage. However, recent experiments suggest that the effects of CO_2 enrichment on ecosystems will be far more complex than conventional single-factor CO_2 manipulation experiments have demonstrated, because additional factors (e.g., changes in temperature, precipitation, and nitrogen availability) interact to alter responses to CO_2 (Shaw et al. 2002, Dukes et al. 2005). Furthermore, scaling from the leaf- and plot-level responses that manipulative experiments reveal to the ecosystem scales that are most relevant to the climate system is extremely challenging. Therefore, we have examined static ecosystem responses to changes in climate alone.

Nevertheless, we speculate that CO_2 fertilization effects could either amplify or dampen the impact of plant migration on biophysical and biogeochemical land-surface responses. If physiological responses to CO_2 enrichment reduce the distances that PFTs need to migrate (e.g., if CO_2 enrichment allows PFTs to continue to thrive in locations that become drier), then responses to CO_2 could reduce the disparity between migration assumptions. Alternatively, CO_2 enrichment may disproportionately benefit those PFTs that are most highly adapted to local climate and may thereby increase disparity between migration assumptions.

We also do not consider transient changes in climate or the dynamics of ecosystem responses, each of which could substantially influence biogeochemical and biophysical characteristics of the land surface. The examination of transient responses will require ecosystem (and climate) models that are capable of projecting dynamic changes. However, the validation studies for vegetation dynamics in IBIS (and other dynamic global vegetation models) are too limited, in our view, to place much confidence in projections of dynamic vegetation change. In contrast, IBIS has been extensively validated for near-equilibrium projections of ecosystem structure and function, including the current distribution of vegetation, NPP, biomass, soil carbon, evapotranspiration, water balance, and leaf area (Foley et al. 1996, Delire and Foley 1999, Kucharik et al. 2000). We therefore developed these simulations to take advantage of the ecosystem model strengths and minimize weaknesses, even at the expense of much-needed understanding of transient ecosystem responses.

Similarly, climate in HadCM3 does not reach equilibrium for the A1FI scenario. Indeed, GHG concentrations do not

reach equilibrium in the A1FI scenario. Therefore, the ecosystem responses examined here are to a fixed climate, whereas the real global climate would keep changing. Our simulation approach also overlooks several potentially important components of climate change, including cloud responses and variability (e.g., changes in temperature range or number of rainy days) that would be likely to accompany the temperature and precipitation changes modeled under the A1FI emissions scenario. Nevertheless, this sensitivity analysis constitutes an important first step by demonstrating that plant migration can heavily influence biophysical and biogeochemical responses to climate change.

Conclusions

Different species, populations, and individuals disperse and migrate at different rates. In at least some cases, biotic responses to the rapid changes in climate expected over the next century will be slow. Here we demonstrate that the effectiveness of plant migration can strongly influence biogeochemical and biophysical responses of the land surface by altering carbon storage, evapotranspiration, and the absorption of solar radiation. This is an important first step in determining future biophysical and biogeochemical characteristics of the land surface. However, future predictions will need to incorporate responses to multiple interacting global changes (physiological CO_2 effects, nitrogen deposition, land-use patterns, and exotic species invasions), a mechanistic treatment of migration, and dynamic coupling of climate and biological systems. Nevertheless, this sensitivity study demonstrates that plausible ranges in migration rates can affect the magnitude, and in some cases the sign, of feedbacks from the land surface to the climate system. Therefore, prediction of future climate depends on developing and incorporating a better understanding of migration.

Acknowledgments

P. A. T. H. thanks the National Science Foundation (DBI-0305907) for funding. Jon Foley, Rik Leemans, and three anonymous reviewers provided valuable comments. Foley and Dierk Polzin from the Center for Sustainability and the Global Environment provided IBIS. We used Ferret, a product of the National Oceanic and Atmospheric Administration's Pacific Marine Environmental Laboratory, for graphics and visualization (*www.ferret.noaa.gov*).

References cited

Betts RA, Cox PM, Lee SE, Woodward FI. 1997. Contrasting physiological and structural vegetation feedbacks in climate change simulations. Nature 387: 796–799.

Chapin FS, et al. 2005. Role of land-surface changes in Arctic summer warming. Science 310: 657–660.

Clark JS. 1998. Why trees migrate so fast: Confronting theory with dispersal biology and the paleorecord. American Naturalist 152: 204–224.

Clark JS, Lewis M, McLachlan JS, HilleRisLambers J. 2003. Estimating population spread: What can we forecast and how well? Ecology 84: 1979–1988.

Collatz GJ, Ball JT, Grivet C, Berry JA. 1991. Physiological and environmental regulation of stomatal conductance, photosynthesis and transpiration: A model that includes a laminar boundary layer. Agricultural and Forest Meteorology 53: 107–136.

Collatz GJ, Ribas-Carbo M, Berry JA. 1992. Coupled photosynthesis–stomatal conductance model for leaves of C_4 plants. Australian Journal of Plant Physiology 19: 519–538.

Cramer W, Kicklighter DW, Bondeau A, Moore B, Churkina G, Nemry B, Ruimy A, Schloss AL. 1999. Comparing global models of terrestrial net primary productivity (NPP): Overview and key results. Global Change Biology 5: 1–15.

Delire C, Foley JA. 1999. Evaluating the performance of a land surface ecosystem model with biophysical measurements from contrasting environments. Journal of Geophysical Research–Atmospheres 104: 16895–16909.

Dukes JS, Chiariello NR, Cleland E, Moore LA, Shaw MR, Thayer S, Tobeck T, Mooney HA, Field CB. 2005. Responses of grassland production to single and multiple global environmental changes. PLoS Biology 3: e319.

Farquhar GD, von Caemmerer S, Berry JA. 1980. A biogeochemical model of photosynthetic CO_2 assimilation in leaves of C_3 species. Planta 149: 78–90.

Feddema JJ, Oleson KW, Bonan GB, Mearns LO, Buja LE, Meehl GA, Washington WM. 2005. The importance of land-cover change in simulating future climates. Science 310: 1674–1678.

Field CB, Avissar R. 1998. Bidirectional interactions between the biosphere and the atmosphere—introduction. Global Change Biology 4: 459–460.

Foley JA, Prentice IC, Ramankutty N, Levis S, Pollard D, Sitch S, Haxeltine A. 1996. An integrated biosphere model of land surface processes, terrestrial carbon balance, and vegetation dynamics. Global Biogeochemical Cycles 10: 603–628.

[GSDTG] Global Soils Data Test Group. 2000. Global Soil Data Products CD-ROM (IGBP-DIS). Oak Ridge (TN): Oak Ridge National Laboratory Distributed Active Archive Center. (3 March 2006; *www.daac.ornl.gov*)

Harte J, Ostling A, Green JL, Kinzig A. 2004. Biodiversity conservation: Climate change and extinction risk. Nature 427: 145–148.

Higgins PAT. 2004. Biogeochemical and biophysical responses of the land surface to a sustained thermohaline circulation weakening. Journal of Climate 17: 4135–4142.

Higgins SI, Richardson DM. 1999. Predicting plant migration rates in a changing world: The role of long-distance dispersal. American Naturalist 153: 464–475.

[IPCC] Intergovernmental Panel on Climate Change. 2001. Climate Change 2001: The Scientific Basis. Contribution of Working Group I to the Third Assessment Report of the Intergovernmental Panel on Climate Change. Cambridge (United Kingdom): Cambridge University Press.

Jobbagy EG, Jackson RB. 2000. The vertical distribution of soil organic carbon and its relation to climate and vegetation. Ecological Applications 10: 423–436.

Johns TC, et al. 2003. Anthropogenic climate change for 1860 to 2100 simulated with the HadCM3 model under updated emissions scenarios. Climate Dynamics 20: 583–612.

Johnstone JF, Chapin FS. 2003. Non-equilibrium succession dynamics indicate continued northern migration of lodgepole pine. Global Change Biology 9: 1401–1409.

Kiehl JT, Trenberth KE. 1997. Earth's annual global mean energy budget. Bulletin of the American Meteorological Society 78: 197–208.

Korner C. 2000. Biosphere responses to CO_2 enrichment. Ecological Applications 10: 1590–1619.

Kucharik CJ, Foley JA, Delire C, Fisher VA, Coe MT, Lenters JD, Young-Molling C, Ramankutty N, Norman JM, Gower ST. 2000. Testing the performance of a Dynamic Global Ecosystem Model: Water balance, carbon balance, and vegetation structure. Global Biogeochemical Cycles 14: 795–825.

Lashof DA, DeAngelo BJ, Saleska SR, Harte J. 1997. Terrestrial ecosystem feedbacks to global climate change. Annual Review of Energy and the Environment 22: 75–118.

Malcolm JR, Markham A, Neilson RP, Garaci M. 2002. Estimated migration rates under scenarios of global climate change. Journal of Biogeography 29: 835–849.

Marland G, Boden TA, Andres RJ. 2003. Global, regional, and national CO_2 emissions. In Carbon Dioxide Information Analysis Center. Trends: A Compendium of Data on Global Change. Oak Ridge (TN): US Department of Energy.

McLachlan JS, Clark JS. 2004. Reconstructing historical ranges with fossil data at continental scales. Forest Ecology and Management 197: 139–147.

Mooney HA, Canadell J, Chapin FSI, Ehleringer JR, Korner C, McMurtrie RE, Parton WJ, Pitelka LF, Schulze ED. 1999. Ecosystem physiology responses to global change. Pages 141–189 in Walker B, Steffen W, Canadell J, Ingram J, eds. The Terrestrial Biosphere and Global Change. Cambridge (United Kingdom): Cambridge University Press.

Nakicenovic N, et al. 2000. IPCC Special Report on Emissions Scenarios. Cambridge (United Kingdom): Cambridge University Press.

Neilson RP, Pitelka LF, Solomon AM, Nathan R, Midgley GF, Fragoso JMV, Lischke H, Thompson K. 2005. Forecasting regional to global plant migration in response to climate change. BioScience 55: 749–759.

New M, Hulme M, Jones P. 1999. Representing twentieth-century space-time climate variability. Part I: Development of a 1961–90 mean monthly terrestrial climatology. Journal of Climate 12: 829–856.

Norby RJ, et al. 2005. Forest response to elevated CO_2 is conserved across a broad range of productivity. Proceedings of the National Academy of Sciences 102: 18052–18056.

Nowak RS, Ellsworth DS, Smith SD. 2004. Functional responses of plants to elevated atmospheric CO_2—do photosynthetic and productivity data from FACE experiments support early predictions? New Phytologist 162: 253–280.

Parmesan C, Yohe G. 2003. A globally coherent fingerprint of climate change impacts across natural systems. Nature 421: 37–42.

Pielke R, Avissar R, Raupach M, Dolman A, Zeng X, Denning A. 1998. Interactions between the atmosphere and terrestrial ecosystems: Influence on weather and climate. Global Change Biology 4: 461–475.

Ramankutty N, Foley JA. 1999. Estimating historical changes in global land cover: Croplands from 1700 to 1992. Global Biogeochemical Cycles 13: 997–1027.

Root TL, Price JT, Hall KR, Schneider SH, Rosenzweig C, Pounds JA. 2003. Fingerprints of global warming on wild animals and plants. Nature 421: 57–60.

Saleska SR, Shaw MR, Fischer ML, Dunne JA, Still CJ, Holman ML, Harte J. 2002. Plant community composition mediates both large transient decline and predicted long-term recovery of soil carbon under climate warming. Global Biogeochemical Cycles 16: 1055.

Sellers PJ, et al. 1997. Modeling the exchanges of energy, water, and carbon between continents and the atmosphere. Science 275: 502–509.

Shaw MR, Zavaleta ES, Chiariello NR, Cleland EE, Mooney HA, Field CB. 2002. Grassland responses to global environmental changes suppressed by elevated CO_2. Science 298: 1987–1990.

Solomon AM, Kirilenko AP. 1997. Climate change and terrestrial biomass: What if trees do not migrate? Global Ecology and Biogeography Letters 6: 139–148.

Tinner W, Lotter AF. 2001. Central European vegetation response to abrupt climate change at 8.2 ka. Geology 29: 551–554.

van Minnen JG, Leemans R, Ihle F. 2000. Defining the importance of including transient ecosystem responses to simulate C-cycle dynamics in a global change model. Global Change Biology 6: 595–611.

Washington WM, Parkinson CL. 1986. An Introduction to Three-Dimensional Climate Modeling. Mill Valley (CA): University Science Books.